Scanning Electrochemical Microscopy. Apparatus and Two-Dimensional Scans of Conductive and Insulating Substrates

Juhyoun Kwak and Allen J. Bard*

Department of Chemistry, The University of Texas, Austin, Texas 78712

The application of scanning electrochemical microscopy (SECM) in the feedback mode to two-dimensional scans over conductive and insulating substrates to obtain topographic information at the micrometer-level is described. In the feedback mode the effect of the conductivity of the substrate and distance of the substrate from a scanning ultramicroelectrode tip on the current flowing at the tip caused by an electrode reaction is recorded as a function of the tip $x-y$ position. Experiments with a 50-μm Pt wire on glass, a ca. 50-μm glass fiber on glass, a gold minigrid, a Pt foil, and a KCl crystal in both aqueous and acetonitrile solutions are presented. The construction of the SECM and the hardware and software that control three-dimensional tip movement and data acquisition are also described.

INTRODUCTION

Recent papers from our group described the principles of scanning electrochemical microscopy (SECM) (*1*) and the quantitative theory of the feedback mode of SECM (*2*). Although the name SECM was not used, similar techniques were also introduced by other groups (*3*, *4*) to study the diffusion layer at electrode surfaces. In SECM an ultramicroelectrode (UME), with a tip radius of the order of micrometers or less, is moved in close proximity to a substrate of interest in contact with a solution containing an electroactive species. The electrode reaction at the tip gives rise to a tip current (i_T) that is affected by the substrate. In general, the tip current, i_T, is controlled by electrochemical reactions at the tip electrode and sample substrate and is a function of the tip/substrate distance, d, and the conductivity and chemical nature of the sample substrate. The measurement of i_T can thus provide the information about sample topography and its electrical and chemical properties. In our previous paper (*1*), we described experiments in which the tip was moved normal to the substrate surface (the z direction) and showed the variation of i_T with d with both insulating and conductive substrates. In the feedback mode, i_T increases when the tip electrode is moved close to a conductive substrate and decreases when the tip electrode is moved close to an insulating substrate. Therefore, contour information about conductive and insulating sample substrates can be obtained by scanning the tip electrode across the surface of the sample substrate (the $x-y$ plane) after the tip has been brought into close proximity of the substrate in the z direction. In this paper we focus on such $x-y$ (topographic) scans of substrates and describe a new instrument for the control and determination of the three-dimensional location of the tip electrode. This instrument was interfaced with a microcomputer for control of the tip position and potential and processing of the acquired data. With this instrument a platinum wire (50 μm diameter) and a glass fiber (ca. 50 μm diameter) mounted on glass slides were scanned to check the instrument performance. Topographic scans of platinum foil, a gold minigrid, and a potassium chloride crystal are also presented. Experiments with both aqueous and nonaqueous (MeCN) solutions of electroactive species are described. All of the results are represented in three-dimensional rectangular coordinates, i.e., the x and y axes show the location of the tip and the z axis shows the tip current (which is a function of tip/substrate distance).

EXPERIMENTAL SECTION

Hardware. The instrument, a scanning electrochemical microscope (also abbreviated SECM), was assembled from commercially available and home-built components. A block diagram of the SECM is shown in Figure 1. The instrument was controlled with a 12-MHz Deskpro 286 microcomputer (Compaq Computer Corp., Houston, TX) equipped with a data acquisition board (DT 2821-G-8DI; Data Translation, Inc., Marboro, MA), which has 8 differential analog input channels (12-bit resolution, 250-kHz throughput), 2 analog output channels (12-bit resolution, 130-kHz throughput), and 16 digital I/O lines. For hard copy, an IBM color printer and HP ColorPro graphics plotter (Hewlett-Packard Corp., San Diego, CA) were used. The electrode potentials were controlled by PAR 175 Universal Programmers (Princeton Applied Research Corp., Princeton, NJ) via a home-built bipotentiostat (*5*, *6*).

The DT 2821-G-8DI board was externally connected to a DT752-Y (signal conditioning screw terminal board; Data Translation, Inc.) to acquire the electrochemical signals via the biopotentiostat, the potential of the piezoelectric device (PZT PZ-44, 0–40 μm; Burleigh Instruments, Inc., Fishers, NY) via a high-voltage dc operational amplifier (Burleigh PZ-70), and the potentials of the piezoelectric devices of the x, y, and z micropositioning devices (Burleigh inchworm translators, IW-500-2 for x and y movement and IW-702-00 for z movement; controlled by modified Burleigh inchworm movement controllers (CE-2000-3A00)). To obtain the analog signals and digital signals from the CE-2000-3A00 (which contains an internal Motorola MC6809 microprocessor), the six boards (two boards for each axis; counter board and controller board) were modified (*6*). These signals were preconditioned with a home-built logic circuit (*6*) connected to a DT752-Y board. The DT 2821-G-8DI was externally connected to a DT709 (signal conditioning screw terminal board; Data Translation, Inc.) to send the analog signal to control the PZT pusher PZ-44 via PZ-70 and receive the digital signals from the modified CE-2000-3A00 via the home-built logic circuit. These digital signals are needed to obtain the three-dimensional location of the tip electrode as well as to move the tip electrode in a programmed mode.

The inchworm translators (IW-500-2 and IW-702-00) were mounted on a stage capable of three-dimensional motion, which was mounted on an optical table with TS-100 Translation and TS-300 z-axis stages (Burleigh Instruments, Inc.). The stainless steel plate with a PZT pusher housing was also attached to this stage, as shown in Figure 2. The tip electrode holder was glued to the ceramic cap of the PZT pusher with Torr Seal (Varian Associates, Inc., Lexington, MA). With this assembly the tip electrode position above the sample substrate was controlled by both the digital movement of inchworm translators and the analog movement of the PZT pusher.

The resolution of the digital movement of the inchworm translators could be adjusted from $^1/_{128}$ of a "click distance" to

0003-2700/89/0361-1794$01.50/0

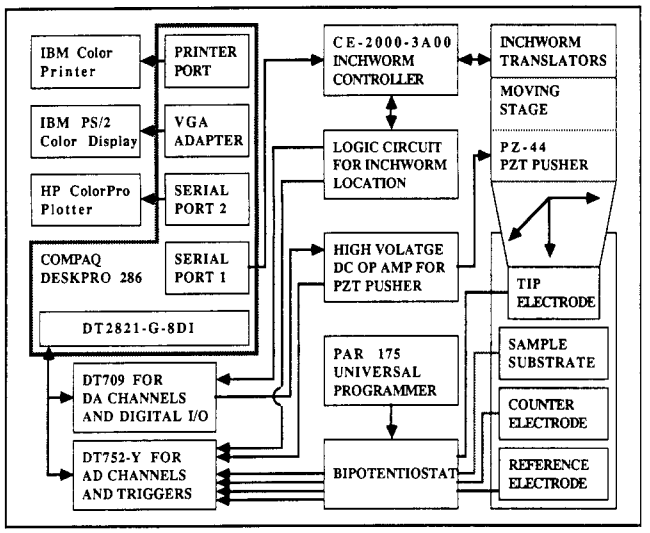

Figure 1. Block diagram of the scanning electrochemical microscope.

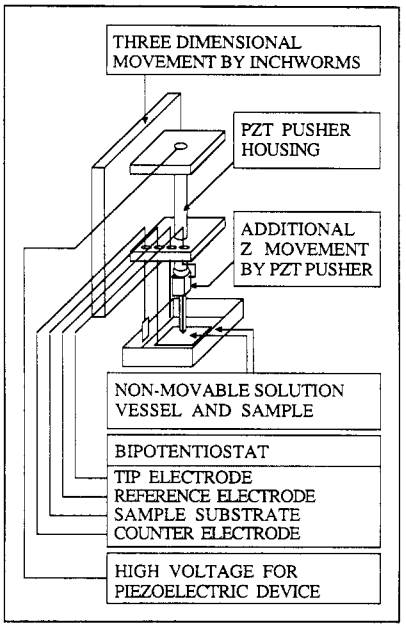

Figure 2. Diagram of electrochemical cell and scanning tip attached to the three-dimensional micropositioning device.

2 "click distances", depending on selection of digital signals from the CE-2000-3A00 (*6*). The motion of the inchworm translator involves a full contraction and expansion of the cylindrical piezoelectric device along the center shaft as well as clamping and unclamping of this shaft at both ends of the cylindrical piezoelectric. At the moment of clamping and unclamping, a "click" sound is generated. This "click distance" was used as a distance unit (1.1–1.2 μm per click, calibrated as described below) in conjunction with the digital counting unit in the computer program.

Software. The hardware was controlled and accessed by the Deskpro 286 via the MS-DOS operating system (Microsoft Disk Operating System version 3.31; Microsoft Corp., Redmond, WA). Programs for this purpose, as well as for data processing, were written in C language and compiled with a Microsoft C Optimizing Compiler (version 5.1; Microsoft Corp.). The ATLAB subroutine library (Data Translation, Inc.) for the DT2821-G-8DI control was incorporated into the programs when necessary (*6*).

Several different programs were employed. The simplest control program (program 1) was used to acquire electrochemical signals through the DT2821-G-8DI while the tip electrode was held stationary. This program allowed the usual electrochemical experiments (cyclic voltammetry, chronoamperometry, chronocoulometry) to be carried out. The acquired data could be saved on a mass storage device (floppy or hard disk) as a file which could be imported by Lotus 1-2-3 (Lotus Development Corp., Cambridge, MA) to be plotted in graphics form.

Another control program (program 2) acquired the electrochemical signals as well as data about the tip location via DT2821-G-8DI, while it also controlled the movement of the tip via the programmed or step mode of the CE-2000-3A00 through a serial port 1 (see Figure 1). The programmed mode allowed a two-dimensional scan over the sample substrate, while the step mode was used to move the tip electrode to the sample substrate or to perform a single scan over the sample substrate before obtaining a two-dimensional scan. The acquired data and control parameters were saved in random access memory, graphically displayed on the monitor screen, and optionally saved on a floppy or hard disk.

A processing program (program 3) was used to convert the data obtained from program 2 to a binary data format, which was adaptable to the commercial Surfer program (Golden Software, Inc., Golden, CO). The Surfer program has many features for data manipulation and presentation, i.e., data smoothing (spline and matrix method), three-dimensional plotting (x, y axis for two-dimensional location and z axis for current at tip electrode) on hard copy devices and monitor, as well as topographic plotting.

Chemicals. Milli-Q reagent water (Millipore Corp., Bedford, WA) was used for the aqueous solutions, with dissolved $K_4Fe(CN)_6$ and KCl, as received. Acetonitrile (MeCN, spectrophotometric grade; Mallinckrodt, Inc., Paris, KY), which was equilibrated with Mallinckrodt molecular sieve (grade 514GT 4 Å), was used for the nonaqueous solutions with various supporting electrolytes: tetrabutylammonium fluoroborate ($TBABF_4$), tetrabutylammonium fluorophosphate ($TBAPF_6$), and tetrabutylammonium perchlorate (TBAP) (Southwestern Analytical Chemicals, Inc., Austin, TX). These were dried overnight in a vacuum oven. Ferrocene (Cp_2Fe; Morton Thiokol, Inc., Danvers, MA) was used as received.

Tip Preparation. Several different tips were used in these experiments. Construction of the Pt disk-in-glass ultramicroelectrode (12.5- and 5-μm radii) has been described previously (*1*). The carbon disk-in-glass ultramicroelectrodes (5.5- and 3.5-μm radii) were made by a similar procedure as the Pt electrodes. The glass surrounding the Pt or C ultramicroelectrodes was conically sharpened after the usual polishing procedure (*1*) to avoid contacting the substrate with the insulating glass sheath.

Sample Preparation. The Pt wire sample was glued on a microscope slide (1 in. × 3 in.) by applying epoxy cement only at both ends of a 1.5 cm long Pt wire (50-μm diameter). The glass fiber (ca. 50 μm diameter) was pulled from a Pyrex glass tube and glued on a microscope slide in the same manner. The Au minigrid (7.6 μm wire width and 17.6 μm hole size; Buckbee-Mears Co., St. Paul, MN) (*7*) was cut as a 2 × 2 mm square and carefully glued to a glass slide only at the edges. The KCl crystals were grown from an aqueous saturated KCl solution. A sample crystal was glued onto a microscope slide. The solution vessel was a Pyrex tube (1 in. o.d., ca. 1 cm long) that was glued on the microscope slide which held the sample.

Scanning of Samples. The microscope slide on which the sample substrate and solution vessel were glued (Figure 2) was placed on a heavy brass plate (3 in. × 5 in. × 0.5 in.), which was held on a manually adjustable tripod. With this tripod, the sample substrate was moved to within about 1 mm of the tip electrode. This tripod was also used to level the sample substrate. After this procedure, the sample was not moved during a scanning experiment. After the electrochemical solution was transferred into the solution vessel, the counter electrode (a 2 cm length, 0.5 mm diameter platinum wire) and an appropriate reference electrode (a saturated calomel electrode for aqueous solutions and oxidized silver wire quasi-reference electrode (AgQRE) for nonaqueous solutions) were inserted. A cyclic voltammogram was obtained (with program 1) to check the tip electrode condition. Then, the potential of tip electrode was set at an appropriate potential, and by using program 2, the tip was advanced toward the sample with the z-axis inchworm monitoring the tip current until it either increased by ca. 10% (for a conductive substrate) or decreased ca. 10% (for the insulating substrate). Then, with the PZT pusher PZ-44 or a slower z-axis inchworm step movement, the appropriate location of the tip electrode from the substrate was adjusted. Finally, an x–y scan was executed by the pro-

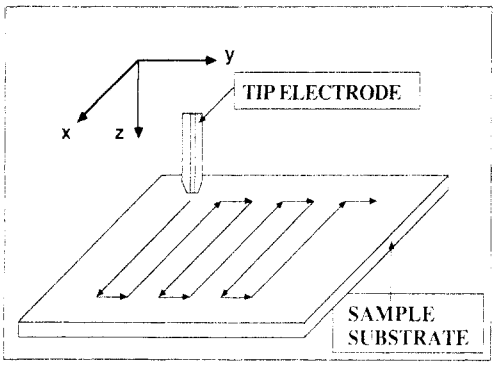

Figure 3. Pattern of two-dimensional movement of tip electrode over the sample substrate.

grammed zigzag movement of x- and y-axis inchworms, as shown in Figure 3.

Calibration. To obtain the absolute position of the tip, it is necessary to calibrate the inchworm drives and PZT pusher. Every micropositioning device is fundamentally based on its piezoelectric material, which has its own dependent parameters (geometric shape, age, load). After the system was setup, with electrode and solution vessel in place, so that the actual load was known, the inchworm of each axis was moved a relatively long distance (i.e., 200 to 4000 "click distances") and that distance was measured with a micrometer. The linearities of all the inchworms were excellent (better than 0.5%), and the following calibrated click distances were obtained: 1.189 μm per click for the x axis, 1.181 μm per click for the y axis, and 1.091 μm per click for the z axis. These values are in good agreement with the nominal company specification, 1.25 μm without load.

To calibrate the z-axis PZT pusher (PZ-44), the SECM feedback mode was used. The tip current was monitored while the tip electrode (5 μm radius Pt disk) was moved toward a planar conductive substrate (a 2.5 mm radius Pt disk) immersed in MeCN containing 5 mM ferrocene and 10 mM TBAP by the z-axis inchworm. The tip movement was stopped when $i_T = i_{T,1}$, which was about 50% larger than i_T when the tip was far from the substrate. The tip was then moved two more clicks toward the substrate with the z-axis inchworm, and the increased current, $i_{T,2}$, was noted. The tip was then moved backward from this location by changing the applied potential of the PZT pusher until the tip current was again equal to $i_{T,1}$. From this experiment, the potential change needed to obtain the same distance as two "click distances" of the z-axis inchworm was obtained, i.e., 26.0 V to the pusher was equivalent to two "click distances" of the z-axis inchworm. Thus, the calibration factor for the PZT pusher was 42.0 μm per 1000 V. This value is also in good agreement with nominal company specification (ca. 40 μm per 1000 V).

RESULTS AND DISCUSSION

Pt Wire on Glass. The i_T values for scans over a 50 μm diameter platinum wire on a glass slide immersed in MeCN/0.01 M TBAP, 5 mM Cp_2Fe, are shown in Figure 4. Four scans for the tip at different locations above the sample (different d values) are shown. The tip electrode was held at 0.8 V vs AgQRE where oxidation of Cp_2Fe to Cp_2Fe^+ occurs. When the tip was far from platinum wire, i_T was independent of d and showed an anodic current of 26.5 ± 0.3 nA that was independent of the x–y position. As previously shown (2), i_T is not affected by the substrate when $d \gg a$ (where a is the tip radius). When the tip was moved closer to the sample (i.e., d decreased), i_T was perturbed from its long distance value ($i_{T,\infty}$). When it was over the glass, $i_T < i_{T,\infty}$, since the insulating substrate partially blocked diffusion of Cp_2Fe to the tip. When the tip was above the Pt wire, $i_T > i_{T,\infty}$, because of the feedback effect, i.e., regeneration of Cp_2Fe at the Pt wire via reduction of Cp_2Fe^+. The maximum anodic currents were 30.6 nA (Figure 4B), 31.3 nA (Figure 4C), and 33.0 nA (Figure 4D). Although the z-axis calibration provides an accurate measurement of the *relative* position above the substrate, one

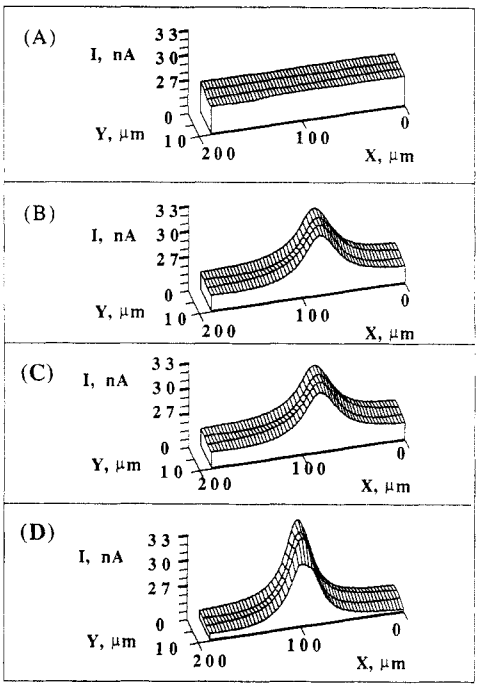

Figure 4. Scans of a 50-μm platinum wire on a glass slide at different tip locations from sample: tip electrode, 5.5 μm radius carbon disk tip electrode at 0.80 V vs AgQRE; solution, 10 mM TBAP, 5 mM ferrocene in acetonitrile; scanning speed, 19.7 μm/s; (A) far from sample, (B) close (about 17.8 μm, see text) to sample, (C) 2.18 μm closer than B, (D) 4.36 μm closer than B.

cannot obtain directly an absolute measure of d. For example, any attempt to move the tip to the substrate until they touch (a "tip crash") would damage both tip and sample. Thus, the best estimate of d can be obtained from the theoretical treatment of the SECM in the feedback mode (2), where the value of $i_T/i_{T,\infty}$ can be related to d/a. Since the theory assumes a planar substrate, the estimated absolute d value can only be considered an approximation when there is appreciable curvature of the substrate or it consists of insulating and conductive zones with dimensions of the order of the tip radius. Both of these conditions apply for the 50 μm Pt wire on glass substrate under consideration here. On the basis of the theoretical treatment, which yields the following approximate (within 2%) equation for a planar conductive substrate (2)

$$(i_T/i_{T,\infty}) = (\pi/4)(a/d) + 0.901 + 0.099 \exp[-0.16(a/d)] - 0.29 \exp[-0.39(d/a)] \quad (1)$$

the maximum anodic currents in Figure 4, for the tip directly over the Pt wire, can be converted to estimated distances, d; the resulting values are 17.8 ± 1.5 μm (Figure 4B), 15.6 ± 1.1 μm (Figure 4C), and 11.8 ± 0.7 μm (Figure 4D). These estimated data are in reasonable agreement with the relative tip location from sample (see figure caption). Note that the errors become smaller as the tip electrode gets closer to the substrate. These nonlinear errors are caused by the intrinsic nonlinearities of tip current vs tip/substrate distance.

Glass Fiber on Glass. Five scans at different tip locations above a glass fiber (ca. 50 μm) on a glass slide are shown in Figure 5. A 5 μm radius Pt tip embedded in a glass sheath and held at 0.50 V vs SCE and immersed in an aqueous 2.5 mM $K_4Fe(CN)_6$, 0.1 M KCl solution was employed. When the tip electrode was far from the substrate, the tip current was constant at 2.08 ± 0.07 nA. When the tip was brought closer to the sample, the hindered diffusion of ferrocyanide to the tip because of the insulating glass fiber and slide caused a decrease in the currents at the tip electrode. The minimum

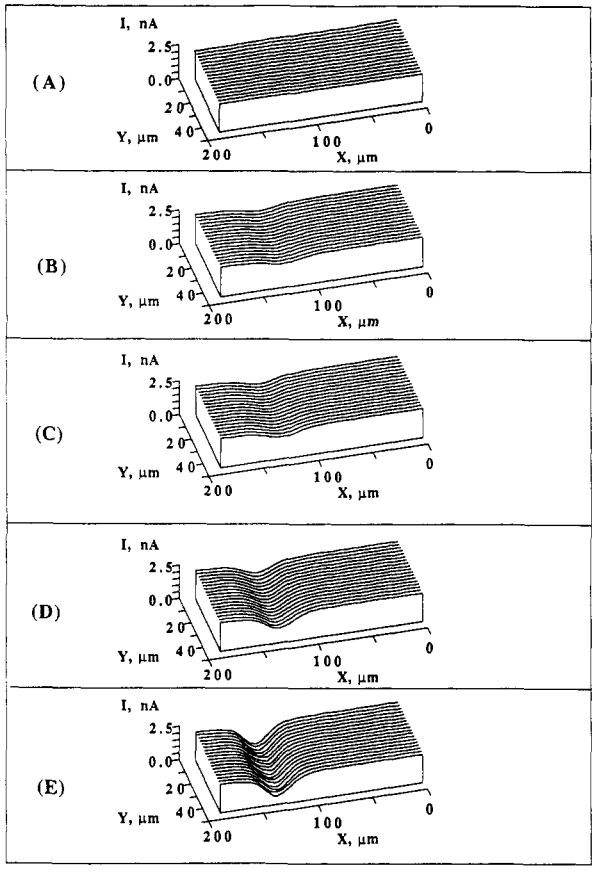

Figure 5. Scans of a ca. 50 μm glass fiber on a glass slide at different tip locations from sample: tip electrode, 5 μm radius platinum disk tip electrode at 0.50 V vs SCE; solution, 0.1 M KCl, 2.5 mM potassium ferrocyanide in H_2O; scanning speed, 25.0 μm/s; (A) far from sample, (B) close (about 8.05 μm, see text) to sample, (C) 2.18 μm closer to sample than B, (D) 4.36 μm closer to sample than B, (E) 6.54 μm closer to sample than B.

anodic currents were 1.74 nA (Figure 5B), 1.60 nA (Figure 5C), 1.06 nA (Figure 5D), and 0.4 nA (Figure 5E). The distance between tip and substrate, d, was again estimated from theory (2); the estimated distances between tip and the top of the glass fiber are 8.05 μm (Figure 5B), 5.87 μm (Figure 5C), 3.68 μm (Figure 5D), and 1.50 μm (Figure 5E). These estimates are in excellent agreement with the calibrated relative movements shown in the figure caption. As we reported previously (2), the radius of glass sheath surrounding the disk electrode affects the tip current. In this case, it was about 10 times that of the disk electrode.

Platinum Foil. To test the SECM with a larger area conductive substrate, scans with a 5 μm radius Pt tip at 0.5 V over a polycrystalline Pt foil immersed in an aqueous 2.5 mM $K_4Fe(CN)_6$, 0.1 M KCl solution were carried out. Two scans are shown in Figure 6. As in the previous experiments, the tip was scanned two dimensionally far from the sample both before (Figure 6A, first scan) and after (sixth scan) the closer scans, yielding constant currents of 2.45 ± 0.09 and 2.32 ± 0.04 nA, respectively. The semiinfinite steady-state diffusion current was found to decrease with time compared to the current obtained at the same freshly polished electrode. Since the steady-state current is an important variable in SECM in the estimation of the absolute tip to substrate distance, all the scans should be executed over a minimum period (e.g., an hour or less) or the tips should be frequently polished, either mechanically or electrochemically. In this experiment the time spent obtaining the six scans was about 20 min over which the semiinfinite steady-state diffusion current decreased by about 5%. When the tip was brought closer to the Pt foil and scanned (second scan), i_T increased to 2.59 ± 0.04 nA. At

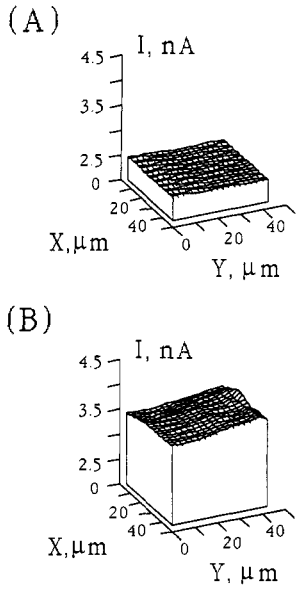

Figure 6. Scans of a platinum foil: tip electrode, 5 μm radius platinum disk tip electrode at 0.50 V vs SCE; solution, 0.1 M KCl, 2.5 mM potassium ferrocyanide in H_2O; scanning speed, 19.7 μm/s; (A) far from sample, (B) close to sample.

this distance information about the surface topography of the foil could not be obtained. When the tip was brought 10.9 μm closer and scanned (third scan), the current increased to 2.89 ± 0.09 nA, still without obtaining contour information. However, with the tip 6.54 μm closer than in the third scan, the increased tip current produced a scan (fourth scan) that showed the surface structure of a tilted Pt foil (Figure 6B). The fifth scan at the same distance as fourth scan was taken to check reproducibility; scanning data of both matched exactly. From the scan data in Figure 6D, and based on the averaged semiinfinite steady-state diffusion current (2.38 nA), the calculated (2) distance between the tip and platinum foil was in the range of 4.55–6.60 μm. The calculated current ranges for the other locations based on the high-resolution data and estimated distances are 2.93–2.84 nA for the second scan and 2.62–2.65 nA for the third scan, in good agreement with the actual results. These calculated current ranges, which are within the range of variation of the experimental data, illustrate why the tip current data at the distances in the second and third scans do not show the topography of the Pt foil. Variation of i_T with d is too small at these distances to show substrate height variations of 2 μm.

Gold Minigrid. Figure 7 shows scans of a gold minigrid immersed in an aqueous solution (5 μm radius Pt tip). In both cases the scans clearly show the minigrid structure. Figure 7A is typical of a scan for a sample whose level was not adjusted well. The average for the periodicity of the grids in both directions is 25.1 ± 1.8 μm, which is in good agreement with the manufacturer's specification (25.2 μm). Since the diameter of the tip disk electrodes was 10, which is bigger than the width of gold lines in the minigrid (7.6 μm), the current change as the tip electrode moved across the gold lines showed a sinusoidal rather than a step shape. Moreover, when the tip electrode was above a hole between the gold grid lines, the current was not smaller than the semiinfinite steady-state diffusion current. This can be explained qualitatively by the cooperative feedback from all lines surrounding the hole to tip electrode. The extent of feedback is smaller, however, than that when the tip is right above the gold lines.

Parts B–D of Figure 7 demonstrate the reproducibility of the scans. Investigating the data quantitatively, we noticed that the maximum anodic current increased from 4.16 nA (first scan, Figure 7B) to 4.39 nA (second scan, 7C) and 4.49 nA

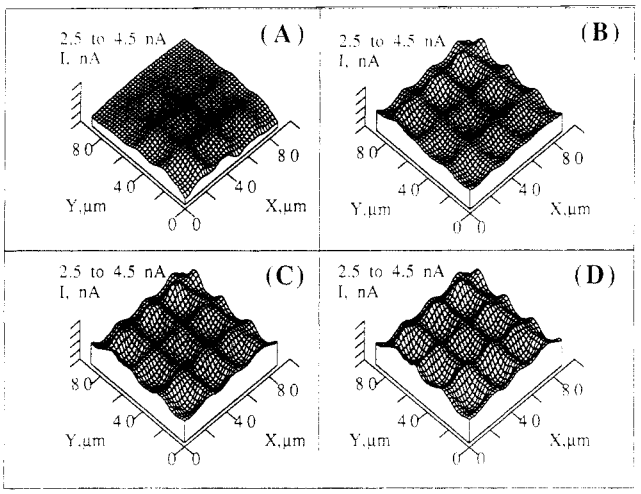

Figure 7. Scans of a gold minigrid: tip electrode, 5 μm radius platinum disk tip electrode at 0.40 V vs SCE; solution, 0.1 M KCl, 2.5 mM potassium ferrocyanide in H_2O; scanning speed, 25.0 μm/s; (A close to sample, first scan, (B) same distance as B, but moved to another section of the minigrid, first scan, (C) same location as B, second scan, (D) same location as B, third scan.

(third scan, 7C), while the minimum anodic current did not change (3.10 ± 0.01 nA). It is difficult to explain these results. Evaporation of the solvent (water) cannot explain them, because only 12 min was required for all of the scans, and also, as discussed above in the Pt foil experiment, the steady-state diffusion current usually decreased with time. It may be that activation (e.g., local electrochemical polishing) occurs at the gold surface, when ferricyanide is reduced back to ferrocyanide. Also, thermal effects of the PZT pusher cannot be excluded. Further studies are needed, however, to understand this effect.

Similar scans were executed in MeCN (5.5 μm radius C tip). In this case, the current increase with time was larger than that in Figure 7, but can mostly be explained by solvent (MeCN) evaporation. Here, the maximum anodic current increased by 11.7% from the first scan to the third scan, while the minimum anodic current also increased by 10.2%. Here, the decrease in the steady-state diffusion current by tip deactivation and the increase of current by gold surface changes, as seen in the aqueous ferrocyanide solution, may have largely cancelled out. The x–y reproducibility of the scans in Figure 7 shows that drifts in these directions (e.g., attributable to thermal effects, hysteresis, and relaxation in the piezoelectric materials, and voltage drifts in the inchworm power supplies) are negligible at this level of resolution over time periods up to 1 h. This suggests that SECM will be useful for examining the same area of an electrode surface with time following different treatments. The reproducibility also shows that neither the electrode tip nor its surrounding glass sheath contacted the sample and dragged it during the scans. All the data in Figure 7 were smoothed before plotting using the matrix average method. In these cases the averaged current at a given x,y grid point was obtained by adding half of the raw current data at that point to half of the averaged currents from the raw data at the eight nearby, x,y grid points. Gray-scale presentation of the data to yield photographic-like images is also possible and is under development.

Potassium Chloride Crystal. To illustrate the use of SECM with an insulating substrate, a KCl crystal immersed in a MeCN solution, where the KCl was insoluble, was examined. The single KCl crystal grows with a spiral pattern on the surface. Since the pattern is not periodic, as is the minigrid, and the surface features are spaced apart (ca. 65 μm), it was difficult to find the desired dislocation steps in a given scan (ca. 100 × 100 μm). Moreover, the protruding apex

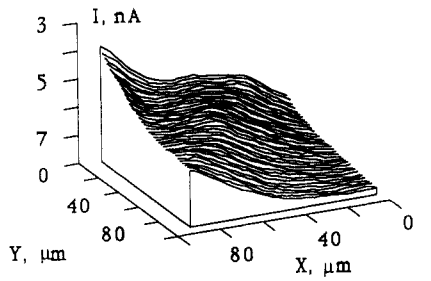

Figure 8. Scan of a KCl crystal: tip electrode, 5 μm radius platinum disk tip electrode at 0.80 V vs AgQRE; solution, 0.01 M TBAP, 2.5 mM ferrocene in acetonitrile; scanning speed, 23.8 μm/s.

crystals, which were detected on the surface of a newly grown crystal, sometimes were removed by collision with the scanning tip electrode. In Figure 8 typical crystal surface steps are shown. In Figure 8A the width between steps can be seen to be about 65 μm, even though the steps are not sharp. Analyzing the data in the same way that the glass fiber results were analyzed, we found one step height of about 2.1 μm (current step from 7.6 to 5.6 nA) and another about 1.6 μm or higher (current step from 7.6 to 3.6 nA). Although these results do not show very good resolution, they do demonstrate the ability of the SECM in the feedback mode to scan, nondestructively, an insulating sample.

CONCLUSIONS

All of the results described above were obtained with the tip scanned at speeds of 7–25 μm/s above the substrate. In all cases the tip currents obtained were considered as steady-state currents, since a theoretical treatment that includes transients and dynamic effects at different scanning speeds is not yet available. Rigorously, only the starting current point of the scan where the tip is held for some time before initiating the x–y raster is at steady state. However, the fact that the current shows no abrupt changes when the scan is initiated, that the currents during the scan over the flat portions of substrate are essentially the same as the starting point current, and that the currents are insensitive to scan speed over this range suggests that the currents found at tips of this size at the spacings used here can be considered as quasi-steady-state currents for scan speeds ≤25 μm/s.

The results presented here clearly demonstrate the application of the SECM to obtain three-dimensional scans and topographic information about conductive and insulating surfaces immersed in liquids at the micrometer-resolution level. The achievement of higher resolution mainly depends upon further developments in tip geometry. For the initial studies described here, little effort was made to minimize tip area or study effects of tip geometry (*1*, *8*). Moreover, the application of mathematical approaches (e.g., a two-dimensional spatial deconvolution) may be of use in improving resolution. A one-dimensional temporal convolution was proposed previously (*9*). Smaller metal tips surrounded by insulators, such as those recently described for use in scanning tunneling microscopy (STM) for samples immersed in liquids (*10*, *11*), might be useful in SECM. For higher resolution scans it will probably be necessary to develop a constant tip current mode, as is frequently used in STM, to avoid crashes of the tip with the surface. In this mode the voltage applied to the z-axis PZT (pusher) is varied to maintain i_T constant at some set value (as different as possible from $i_{T,\infty}$). Information about z-axis displacement is then obtained from plots of the pusher voltage with x and y displacement. While it is very unlikely that SECM will ever attain the atomic resolution found with the STM, submicrometer to 100-Å levels should be possible. For example, the SECM has already been used to deposit

metals with resolution of about 2000 Å (*12*, *13*).

Several other aspects of the SECM are of interest. The ability to study insulators (shared with the atomic force microscope (AFM) (*14*)) should be of use, for example, in the study of the electrodeposition of insulating features on electrode or in insulator/conductor composites. With further development the SECM should be capable of resolving features and producing images of insulating materials (including biological materials) immersed in liquids with a resolution approaching that of the scanning electron microscope. SECM is unique in its ability to distinguish between insulating and conductive regions by reference to the tip current at long distance ($i_{T,\infty}$). Note that no such reference level exists with the STM or AFM. Moreover, a straightforward and well-developed theoretical approach to calculation of normalized tip current as a function of the tip/substrate distance is available (*2*). Not only can SECM provide information about the conductivity of the substrate, it should also be possible, by proper selection of solution redox species, to obtain chemical information (e.g., redox potential) about the substrate. For example, the addition of several electroactive species to the solution which span a range of redox potentials and control of the tip potential should allow one to characterize redox-active sites or species on or in an insulating substrate. These aspects of SECM are currently under investigation in this laboratory.

Registry No. Au, 7440-57-5; Pt, 7440-06-4; KCl, 7447-40-7.

LITERATURE CITED

(1) Bard, A. J.; Fan, F.-R. F.; Kwak, J.; Lev, O. *Anal. Chem.* **1989**, *61*, 132-138.
(2) Kwak, J.; Bard, A. J. *Anal. Chem.* **1989**, *61*, 1221-1227.
(3) Engstrom, R. C.; Webber, M.; Wunder, D. J.; Burgess, R.; Winquist, S. *Anal. Chem.* **1986**, *58*, 844-848.
(4) Engstrom, R. C.; Meany, T.; Tople, R.; Wightman, R. M. *Anal. Chem.* **1987**, *59*, 2005-2010.
(5) Bard, A. J.; Faulkner, L. R. *Electrochemical Methods, Fundamentals and Applications*; Wiley: New York, 1980; p 567.
(6) Kwak, J. Ph.D. Dissertation, The University of Texas at Austin, 1989.
(7) Heineman, W. R.; Hawkridge, F. M.; Blount, H. N. In *Electroanalytical Chemistry*; Bard, A. J., Ed.; Marcel Dekker: New York, 1984; Vol. 13.
(8) Engstrom, R. C.; Wightman, R. M.; Kristensen, E. W. *Anal. Chem.* **1988**, *60*, 652-656.
(9) Davis, J. M.; Fan, F.-R. F.; Bard, A. J. *J. Electroanal. Chem.* **1987**, *238*, 9-31.
(10) Gewirth, A. A.; Craston, D. H.; Bard, A. J. *J. Electroanal. Chem.* **1989**, *261*, 477-482.
(11) Penney, R. M.; Heben, M. J.; Lewis, N. S., submitted for publication in *Anal. Chem.*
(12) Hüsser, O. E.; Craston, D. H.; Bard, A. J. *J. Vac. Sci. Technol. B* **1988**, *6*, 1873-1876.
(13) Hüsser, O. E.; Craston, D. H.; Bard, A. J., submitted for publication in *J. Electrochem. Soc.*
(14) Binnig, G.; Quate, C. F.; Gerber, C. *Phys. Rev. Lett.* **1986**, *56*, 930-933.

RECEIVED for review February 6, 1989. Accepted May 25, 1989. The support of this research by the Robert A. Welch Foundation and Texas Advanced Research Program is gratefully acknowledged.

Poly(2-vinylpyrazine) as a Soluble Polymeric Ligand and as an Electrode Coating. Reactions with Pentacyanoferrate(II)

Paolo Ugo[1] and Fred C. Anson*

Arthur Amos Noyes Laboratories, Division of Chemistry and Chemical Engineering, California Institute of Technology, Pasadena, California 91125

The rate and extent of reaction between $H_2OFe(CN)_5^{3-}$ and poly(2-vinylpyrazine) (PVPz) in homogeneous aqueous solutions have been measured and compared with those for the reaction between the corresponding monomeric species ($H_2OFe(CN)_5^{3-}$ and pyrazine). The significant differences observed are attributed to the increasingly negative charge that accumulates on the polymer-metal complex as the reaction proceeds. Solutions of $PVPz(Fe(CN)_5^{3-})_n$ exhibit almost no electrochemical responses in 0.1 M supporting electrolytes but in 1 M solutions a clear response is evident. Stable electroactive coatings of $PVPz(Fe(CN)_5^{3-})_n$ on electrode surfaces can be prepared by exposing cross-linked deposits of PVPz to aqueous solutions of $H_2OFe(CN)_5^{3-}$. The apparent formal potentials of the redox groups in such coatings vary with the concentration of the supporting electrolyte in the way expected for cation permselective membranes. With homogeneous solutions of PVPz about 30% of the pyrazine groups could be coordinated to $-Fe(CN)_5^{3-}$ anions but the maximum extent of binding of $-Fe(CN)_5^{3-}$ to cross-linked coatings of PVPz was only about half as large.

* Author to whom correspondence should be addressed.
[1] Permanent address: Dipartimento di Chimica Fisica, Universita Di Venezia, Calle Larga S. Marta 2137, 30123 Venezia, Italy.

Electrochemical studies of polymer-metal complexes adsorbed, or otherwise attached, to electrode surfaces are prominent in research on chemically modified electrodes (*1-4*). The electrochemistry of soluble polymer-metal complexes has been examined in a few studies (*5*, *6*) but systematic comparisons of the behavior of the same polymer-metal complex when in solution and when attached to electrode surfaces are relatively rare (*6*). Such comparisons could be useful in judging the effects of attachment on the thermodynamics and kinetic behavior of polymer-metal complexes. One problem that must be overcome in order to carry out comparisons of this type is the instability of electrode coatings prepared from polymer-metal complexes that are soluble in the solvent employed. In this study a water-soluble polymer of 2-vinylpyrazine was reacted with pentacyanoferrate(II) to prepare a soluble polymer-metal complex whose electrochemical and spectroscopic behavior were examined. Stable coatings of the polymer were prepared on electrode surfaces by reacting the 2-vinylpyrazine with dibromohexane to quaternize a small percentage of the nitrogen sites and effectively cross-link the coatings, as described by previous workers (*7*, *8*). The resulting coatings were then readily metalated by exposure to solutions of $H_2OFe(CN)_5^{3-}$. The versatility of pyrazine as a very weakly basic but effective ligand for back-bonding metals (*9*) was advantageous because competition with protons for the co-

0003-2700/89/0361-1799$01.50/0